U.S. DEPARTMENT OF THE INTERIOR
U.S. GEOLOGICAL SURVEY

EARTHQUAKE SUMMARY MAP

Prepared in cooperation with the Global Seismographic Network

M6.0 Camposanto, Italy Earthquake of 20 May 2012

Tectonic Setting

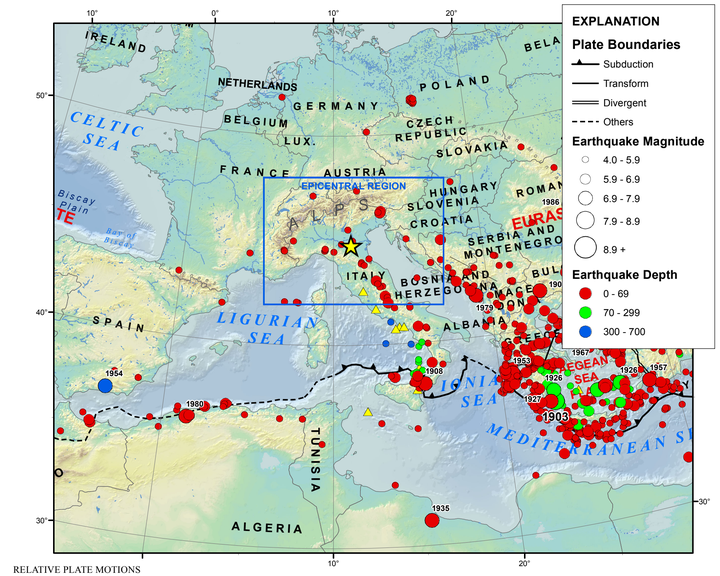

RELATIVE PLATE MOTIONS

The Africa Plate is moving north-northwestward relative to the Eurasia Plate at a rate of about 7 mm/yr.

Seismic Hazard

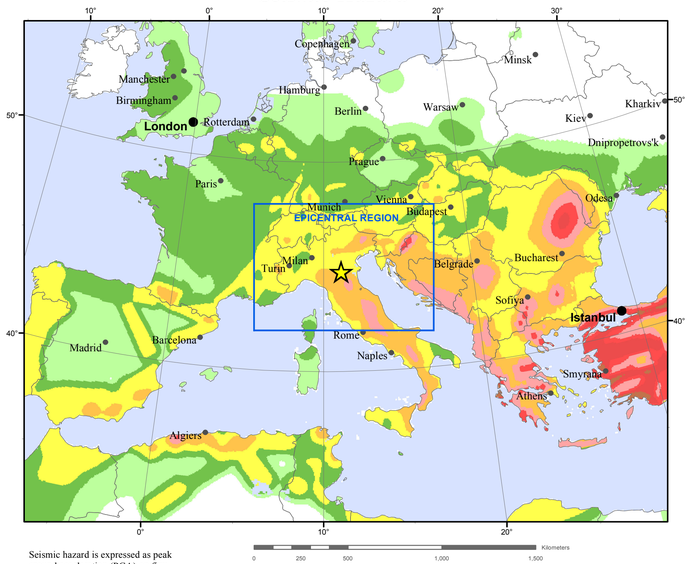

Peak Ground Acceleration in m/sec**2

.2 .4 .8 1.6 2.4 3.2 4.0 4.8

Seismic hazard is expressed as peak ground acceleration (PGA) on firm rock, in meters/sec², expected to be exceeded in a 50-yr period with a probability of 10 percent.

Epicentral Region

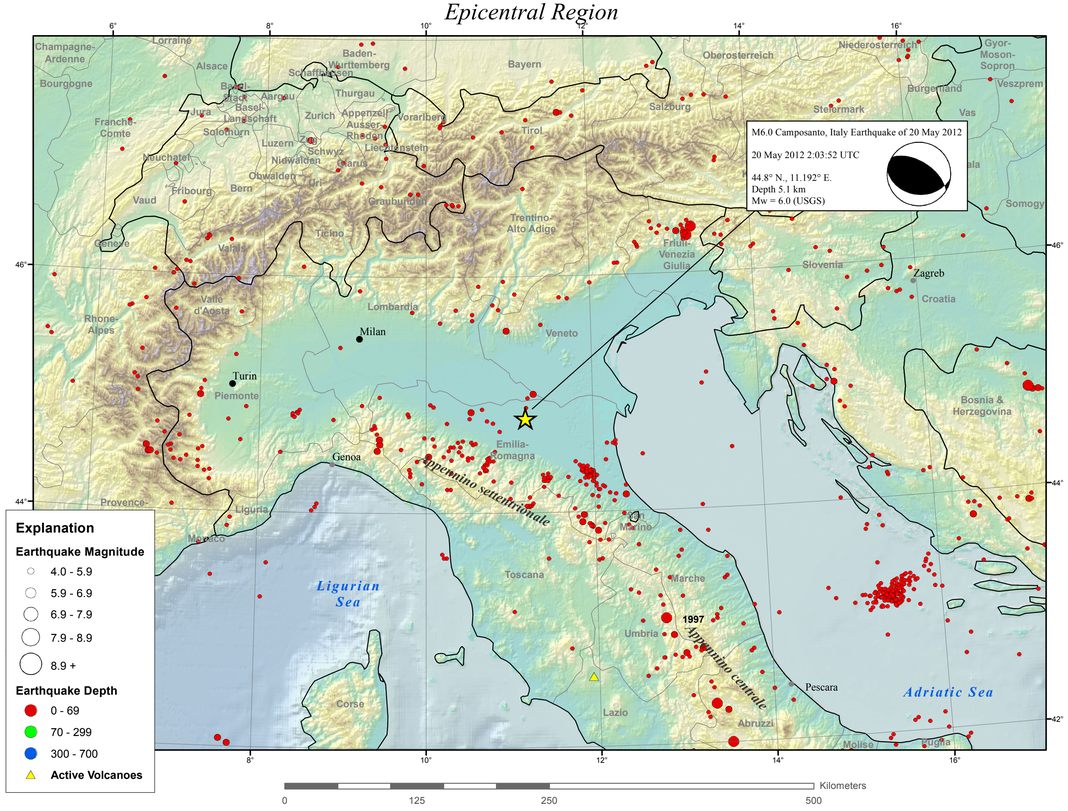

DISCLAIMER

Base map data, such as place names and political boundaries, are the best available but may not be current or may contain inaccuracies and therefore should not be regarded as having official significance.

PAGER

M 6.0, NORTHERN ITALY
Origin Time: Sun 2012-05-20 02:03:52 UTC (04:03:52 local)
Location: 44.80°N 11.19°E Depth: 5 km

Earthquake Shaking — Orange Alert

PAGER Version 6
Created: 13 hours, 12 minutes after earthquake

Estimated Fatalities

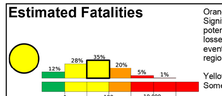

Orange alert level for economic losses. Significant damage is likely and the disaster is potentially widespread. Estimated economic losses are less than 1% of GDP of Italy. Past events with this alert level have required a regional or national level response.

Yellow alert level for shaking-related fatalities. Some casualties are possible.

Estimated Economic Losses

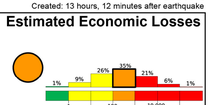

Estimated Population Exposed to Earthquake Shaking

ESTIMATED POPULATION EXPOSURE (k = x1000)		- -*	11,864k*	5,882k	961k	238k	56k	0	0	0
ESTIMATED MODIFIED MERCALLI INTENSITY		I	II-III	IV	V	VI	VII	VIII	IX	X+
PERCEIVED SHAKING		Not felt	Weak	Light	Moderate	Strong	Very Strong	Severe	Violent	Extreme
POTENTIAL DAMAGE	Resistant Structures	none	none	none	V. Light	Light	Moderate	Moderate/Heavy	Heavy	V. Heavy
	Vulnerable Structures	none	none	none	Light	Moderate	Moderate/Heavy	Heavy	V. Heavy	V. Heavy

*Estimated exposure only includes population within the map area.

Population Exposure

population per ~1 sq. km from Landscan

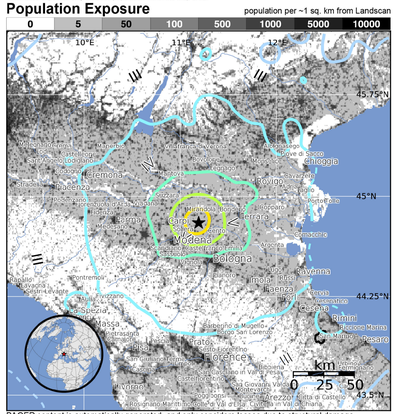

Structures:
Overall, the population in this region resides in structures that are a mix of vulnerable and earthquake resistant construction. The predominant vulnerable building types are unreinforced brick with mud and mid-rise nonductile concrete frame with infill construction.

Historical Earthquakes (with MMI levels):

Date (UTC)	Dist. (km)	Mag.	Max MMI(#)	Shaking Deaths
1997-09-26	230	6.0	VIII(10k)	11
1997-09-26	236	5.7	VIII(2k)	14
1976-05-06	237	6.5	IX(55k)	965

Recent earthquakes in this area have caused secondary hazards such as landslides that might have contributed to losses.

Selected City Exposure

from GeoNames.org

MMI	City	Population
VII	Camposanto	3k
VII	Medolla	6k
VII	Finale Emilia	15k
VI	Ravarino	5k
VI	Crevalcore	12k
IV	Bologna	371k
III	Trento	105k
III	Venice	271k
III	Florence	372k
III	San Marino	29k

bold cities appear on map (k = x1000)

PAGER content is automatically generated, and only considers losses due to structural damage. Limitations of input data, shaking estimates, and loss models may add uncertainty.
http://earthquake.usgs.gov/pager

Event ID: usb0009tk0

TECTONIC SUMMARY

The May 20, 2012 M6.0 earthquake in northern Italy occurred as a result of shallow thrust faulting. At this location, the geology is dominated by compressional tectonics forming thrust-belt type structures like the Apennine Mountains that dominate the Italian peninsula.

The broader Mediterranean region is seismically active due to the northward convergence (4-10 mm/yr) of the African plate with respect to the Eurasian plate along a complex plate boundary. This convergence began approximately 50 Ma and was associated with the closure of the Tethys Sea. The modern day remnant of the Tethys Sea is the Mediterranean Sea. The highest rates of seismicity in the Mediterranean region are found along the Hellenic subduction zone of southern Greece, along the North Anatolian Fault Zone of western Turkey and the Calabrian subduction zone of southern Italy. Local high rates of convergence at the Hellenic subduction zone (35mm/yr) are associated with back-arc spreading throughout Greece and western Turkey above the subducting Mediterranean oceanic crust. Crustal normal faulting throughout this region is a manifestation of extensional tectonics associated with the back-arc spreading. The region of the Marmara Sea is a transition zone between this extensional regime, to the west, and the strike-slip regime of the North Anatolian Fault Zone, to the east. The North Anatolian Fault accommodates much of the right-lateral horizontal motion (23-24 mm/yr) between the Anatolian micro-plate and Eurasian plate as the Anatolian micro-plate is being pushed westward to further accommodate closure of the Mediterranean basin caused by the collision of the African and Arabian plates in southeastern Turkey. Subduction of the Mediterranean Sea floor beneath the Tyrrhenian Sea at the Calabrian subduction zone causes a significant zone of seismicity around Sicily and southern Italy. Active volcanoes are located above intermediate depth earthquakes in the Cyclades of the Aegean Sea and in southern Italy.

In the Mediterranean region there is a written record, several centuries long, documenting pre-instrumental seismicity (pre-20th century). Earthquakes have historically caused widespread damage across central and southern Greece, Cyprus, Sicily, Crete, the Nile Delta, Northern Libya, the Atlas Mountains of North Africa and the Iberian Peninsula. The 1903 M8.2 Kythera earthquake and the 1926 M7.8 Rhodes earthquakes are the largest instrumentally recorded Mediterranean earthquakes, both of which are associated with subduction zone tectonics. Between 1939 and 1999 a series of devastating M7+ strike-slip earthquakes propagated westward along the North Anatolian Fault Zone, beginning with the 1939 M7.8 Erzincan earthquake on the eastern end of the North Anatolian Fault system. The 1999 M7.6 Izmit earthquake, located on the westward end of the fault, struck one of Turkey's most densely populated and industrialized urban areas killing, more than 17,000 people. Although seismicity rates are comparatively low along the northern margin of the African continent, large destructive earthquakes have been recorded and reported from Morocco in the western Mediterranean, to the Dead Sea in the eastern Mediterranean. The 1980 M7.3 El Asnam earthquake was one of Africa's largest and most destructive earthquakes within the 20th century.

Large earthquakes throughout the Mediterranean region have also been known to produce significant and damaging tsunamis. One of the more prominent historical earthquakes within the region is the Lisbon earthquake of November 1, 1755, whose magnitude has been estimated from non-instrumental data to be about 8.0. The 1755 Lisbon earthquake is thought to have occurred within or near the Azores-Gibraltar transform fault, which defines the boundary between the African and Eurasian plates off the west coast of Morocco and Portugal. The earthquake is notable for both a large death toll of approximately 60,000 people and for generating a tsunami that swept up the Portuguese coast inundating coastal villages and Lisbon. An earthquake of approximately M8.0 near Sicily in 1693 generated a large tsunami wave that destroyed numerous towns along Sicily's east coast. The M7.2 December 28, 1908 Messina earthquake is the deadliest documented European earthquake. The combination of severe ground shaking and a local tsunami caused an estimated 60,000 to 120,000 fatalities.

Significant Earthquakes Mag >= 5.5

Year	Mon	Day	Time	Lat	Long	Dep	Mag
1915	01	13	0652	42.000	13.500	0	6.9
1969	10	26	1536	44.807	17.353	15	5.6
1969	10	27	0810	44.837	17.234	15	6.1
1976	05	06	2000	46.385	13.266	20.9	6.5
1976	09	11	1631	46.337	13.181	4.2	5.5
1976	09	15	0315	46.314	13.206	0.9	6.0
1976	09	15	0921	46.351	13.086	9.3	5.9
1979	09	19	2135	42.773	13.010	15	5.9
1984	05	07	1749	41.737	13.891	21.5	5.9
1997	09	26	0940	43.078	12.790	6	6.0
1997	10	14	1523	42.931	12.876	13.8	5.6
2002	10	31	1032	41.789	14.872	10	5.9
2003	03	29	1742	43.109	15.464	10	5.5
2009	04	06	0132	42.334	13.334	8	6.3
2009	04	07	1747	42.275	13.464	15	5.5
2012	05	20	0204	44.8	11.192	5.1	6.0

DATA SOURCES

EARTHQUAKES AND SEISMIC HAZARD
USGS, National Earthquake Information Center
NOAA, National Geophysical Data Center
IASPEI, Centennial Catalog (1900 - 1999) and extensions (Engdahl and Villaseñor, 2002)
HDF (unpublished earthquake catalog) (Engdahl, 2003)
Global Seismic Hazard Assessment Program

PLATE TECTONICS AND FAULT MODEL
PB2002 (Bird, 2003)
Finite Fault Model, Chen Ji, UC Santa Barbara (2007)

BASE MAP
NIMA and ESRI, Digital Chart of the World
USGS, EROS Data Center
NOAA GEBCO and GLOBE Elevation Models

REFERENCES

Bird, P., 2003, An updated digital model of plate boundaries: Geochem. Geophys. Geosyst., v. 4, no. 3, pp. 1027- 80.

Engdahl, E.R. and Villaseñor, A., 2002, Global Seismicity: 1900 - 1999, chap. 41 of Lee, W.H.K., and others,eds., International Earthquake and Engineering Seismology, Part A: New York, N.Y., Elsevier Academeic Press, 932 p.

Engdahl, E.R., Van der Hilst, R.D., and Buland, R.P., 1998, Global teleseismic earthquake relocation with improved travel times and procedures for depth determination: Bull. Seism. Soc. Amer., v. 88, p. 722-743.

Olson, D. M, et.al.,. 2001. Terrestrial Ecoregions of the World: A New Map of Life on Earth. BioScience 51:933-938

Map prepared by U.S. Geological Survey
National Earthquake Information Center
20 May 2012
Map not approved for release by Director USGS